An energy approach for the active vibration control of an oscillator with two translational degrees of freedom using two auxiliary rotating masses

An energy approach for the active vibration control of an oscillator with two translational degrees of freedom using two auxiliary rotating masses

Richard Bäumer, Richard Terrill and Uwe Starossek

Structural Analysis and Steel Structures Institute, Hamburg University of Technology, 21073 Hamburg, Germany

Email: richard.baeumer@tu-harburg.de

Abstract. An active mass damper implementing two auxiliary masses rotating about a single axis is presented. This device is used for the vibration control of an oscillator performing translational motion in a plane (two translational degrees of freedom). In a preferred mode of operation, both auxiliary masses rotate with the same constant angular velocity in opposite directions. The resultant of the produced harmonic centrifugal forces is used for the vibration control. The direction of this control force can be altered by slightly varying the angular velocity of the auxiliary masses. Using an energy approach, a control algorithm was derived. The control algorithm ensures that the control force effectively damps the oscillator when it is displaced in a single, arbitrary direction. Numerical simulations were performed, showing that the presented device with the corresponding control algorithm effectively damps the vibrations on the oscillator.

1. Introduction

High-rise buildings oscillate in both the windward and leeward directions [1]. If the amplitude of these vibrations becomes too large, the occupants of the upper stories of the building may become uneasy. Such vibration-induced problems are not only restricted to high-rise buildings. The wind induced vibrations of monopile wind turbine towers also occur simultaneously in two degrees of freedom [2], leading to increased material fatigue. The first vibration mode mainly determines the motion of such cantilever structures. This motion can be approximated using the oscillator introduced in the following section. To counter these phenomena, an active mass damping device for the vibration control of an oscillator with two translational degrees of freedom has been developed. The centrifugal forces created by the rotational motion of two auxiliary masses is implemented for the vibration control. A similar device, the twin rotor damper (TRD), has been shown to be effective for damping vibrations of oscillators with a single degree of freedom [3], [4], [5]. To ensure power and energy efficiency, the TRD is required to operate in a preferred mode of operation in which both auxiliary masses rotate in opposite directions with the same constant angular velocities. The same principle is now used for the vibration control of an oscillator with two translational degrees of freedom. An energy approach is

used to derive the control algorithm, which is then tested for free vibrations in open-loop configuration analytically and in closed-loop configuration numerically.

2. **Oscillator with two translational degrees of freedom and damping device**

2.1. Oscillator with two translational degree of freedom

The two degree of freedom (TDOF) oscillator is shown in figure 1. The rotational degree of freedom will be neglected. For a free vibration, the motion of the TDOF oscillator in x and y direction is described by equation (1), in which $m + m_c$ is the total mass of the TDOF oscillator, m_c is the mass of both auxiliary masses, k is the spring stiffness, and c is the damping coefficient. The indices denote the degree of freedom and the dot operator indicates a derivative with respect to time.

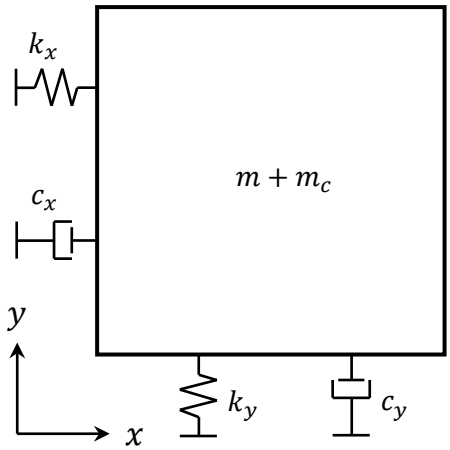

Figure 1: Oscillator with two translational degrees of freedom.

$$(m + m_c)\ddot{x} + c_x\dot{x} + k_x x = 0 \qquad (m + m_c)\ddot{y} + c_y\dot{y} + k_y y = 0 \qquad (1)$$

The spring stiffnesses k_x and k_y and the damping coefficients c_x and c_y are considered to be equal in each direction. Therefore, these indices will be dropped. The natural circular frequency ω_0 and the damping ratio ζ are given by equations (2) and (3), respectively. The damped natural circular frequency of the system ω and the natural period of the TDOF oscillator are given by equation (4) [6]. Assuming that the spring stiffnesses and damping coefficients of TDOF oscillator are equal, the response of the oscillator in each direction is equivalent. Consequently, the control algorithm derived hereinafter is confined to such oscillators. Furthermore, inherent damping is neglected as it only leads to a more complex derivation of the control algorithm without providing additional insight.

$$\omega_0 = \left(\frac{k}{m + m_c}\right)^{1/2} \qquad (2)$$

$$\zeta = \frac{c}{2(m + m_c)\omega_0} \qquad (3)$$

$$\omega = \omega_0(1 - \zeta^2)^{1/2} \qquad T_n = \frac{2\pi}{\omega_0} \qquad (4)$$

2.2. Damping device and control force

The active mass damping device implemented for the vibration control of the TDOF oscillator is shown in figure 2. The device consists of two auxiliary masses $0.5m_c$ connected to a single axis by a massless rod with the length r. The rotors (control mass with massless rod) can move independently

from each other. The angular position of each rotor, $\varphi_1(t)$ and $\varphi_2(t)$, is measured from the positive y-axis, whereas t denotes the time dependency.

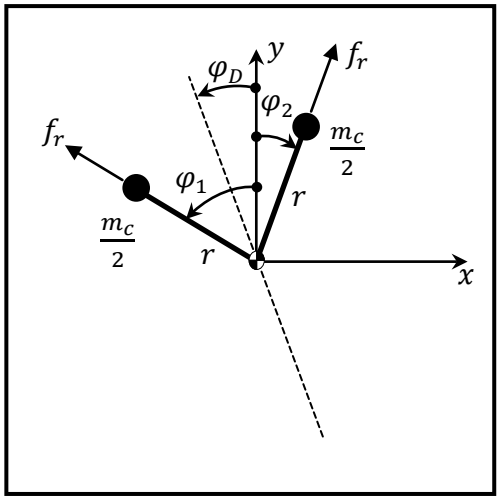

Figure 2: Damping device.

In a preferred mode of operation, each rotor rotates in opposite directions with the same constant angular velocity $\dot{\varphi}$. Therefore, the angular positions are defined by equation (5), in which φ_{01} and φ_{02} are the initial angular positions. Due to the constant angular velocity $\dot{\varphi}$, only the radial force (centrifugal force) given by equation (6) is produced by each rotor. Separating these forces into their x and y components, equations (7) and (8) are formed. The resultant of these two forces defines the control force used for the active vibration control. The direction of this control force, φ_D, solely depends on the initial angular positions, see equation (9). To alter φ_D, the relative angular position between the rotors must be varied, hence changing the angular velocities. This requires unique angular accelerations $\ddot{\varphi}_1$ and $\ddot{\varphi}_2$, ergo tangential forces (normal to the radial forces) in x and y direction, given by equations (10) and (11), are additionally produced. Note, in this case, the no longer constant angular velocities need to be considered in equations (7) and (8).

$$\varphi_1(t) = \dot{\varphi}t + \varphi_{01} \qquad \varphi_2(t) = \dot{\varphi}t + \varphi_{02} \tag{5}$$

$$f_r = \frac{m_c}{2} r\dot{\varphi}^2 \tag{6}$$

$$f_{rx}(t) = \frac{m_c}{2} r\dot{\varphi}^2[\sin(\dot{\varphi}t + \varphi_{02}) - \sin(\dot{\varphi}t + \varphi_{01})] \tag{7}$$

$$f_{ry}(t) = \frac{m_c}{2} r\dot{\varphi}^2[\cos(\dot{\varphi}t + \varphi_{02}) + \cos(\dot{\varphi}t + \varphi_{01})] \tag{8}$$

$$\varphi_D = \frac{\varphi_{01} - \varphi_{02}}{2} \tag{9}$$

$$f_{tx}(t) = \frac{m_c}{2} r(\ddot{\varphi}_1 \cos\varphi_1 - \ddot{\varphi}_2 \cos\varphi_2) \tag{10}$$

$$f_{ty}(t) = \frac{m_c}{2} r(\ddot{\varphi}_1 \sin\varphi_1 + \ddot{\varphi}_2 \sin\varphi_2) \tag{11}$$

3. **Control algorithm**

3.1. Energy approach to ensure maximum damping action

The simplified equations of motion given by equation (12) are derived from equation (1) by dividing it by $(m + m_c)$ and inserting equation (2) into (1) while neglecting inherent damping. Solving these

equations of motion, under the assumption that the effect of the control force on the motion is small, for the displacement response of the TDOF oscillator yields equation (13), whereas the index 0 denotes the initial states [6]. The velocity response of the TDOF oscillator is given by the time derivative of equation (13) seen in equation (14). The control force is required to damp the motion described by this equation. Therefore, the angular velocity of the rotors is set equal to ω_0 and the damping device is operating in the preferred mode of operation. In equation (15), the power of the control force in each direction is given. Integrating equation (15) from $t = 0$ to $t = 2\pi l\omega_0^{-1}$ yields the work done by the control force in each direction on the TDOF oscillator for l vibration cycles, see equation (16). The total work done by the control force is the sum of the work done by it in x and y direction as seen in equation (17). The control force is used to dissipate energy from the oscillator, therefore when the energy in equation (17) is minimal, maximum damping action is achieved.

$$\ddot{x} + \omega_0^2 x = 0 \qquad \ddot{y} + \omega_0^2 y = 0 \tag{12}$$

$$x(t) = x_0 \cos(\omega_0 t) + \frac{\dot{x}_0}{\omega_0}\sin(\omega_0 t) \qquad y(t) = y_0 \cos(\omega_0 t) + \frac{\dot{y}_0}{\omega_0}\sin(\omega_0 t) \tag{13}$$

$$\dot{x}(t) = \dot{x}_0 \cos(\omega_0 t) - x_0\omega_0 \sin(\omega_0 t) \qquad \dot{y}(t) = \dot{y}_0 \cos(\omega_0 t) - y_0\omega_0 \sin(\omega_0 t) \tag{14}$$

$$P_x(t) = f_{rx}(t)\dot{x}(t) \qquad P_y(t) = f_{ry}(t)\dot{y}(t) \tag{15}$$

$$\Delta E_x = \int_0^{\frac{2l\pi}{\omega_0}} f_{rx}(t)\dot{x}(t)dt = \frac{1}{2}m_c r l\omega_0\pi[\dot{x}_0(\sin\varphi_{02} - \sin\varphi_{01}) + x_0\omega_0(\cos\varphi_{01} - \cos\varphi_{02})] \tag{16}$$

$$\Delta E_y = \int_0^{\frac{2l\pi}{\omega_0}} f_{ry}(t)\dot{y}(t)dt = \frac{1}{2}m_c r l\omega_0\pi[\dot{y}_0(\cos\varphi_{01} + \cos\varphi_{02}) + y_0\omega_0(\sin\varphi_{01} + \sin\varphi_{02})]$$

$$\Delta E = \Delta E_x + \Delta E_y \tag{17}$$

Equation (17) is a function of the initial angular positions φ_{01} and φ_{02}. The extrema of equation (17) are identified by setting its partial derivatives with respect to each initial angular position equal to zero, see equations (18) and (19). Solving these equations for the initial angular positions yields equations (20) and (21).

$$\frac{\partial\Delta E}{\partial\varphi_{01}} = \frac{1}{2}m_c r\omega_0\pi l(-\dot{x}_0\cos\varphi_{01} - x_0\omega_0\sin\varphi_{01} - \dot{y}_0\sin\varphi_{01} + y_0\omega_0\cos\varphi_{01}) = 0 \tag{18}$$

$$\frac{\partial\Delta E}{\partial\varphi_{02}} = \frac{1}{2}m_c r\omega_0\pi l(\dot{x}_0\cos\varphi_{02} + x_0\omega_0\sin\varphi_{02} - \dot{y}_0\sin\varphi_{02} + y_0\omega_0\cos\varphi_{02}) = 0 \tag{19}$$

$$\varphi_{01} = \tan^{-1}\frac{-\dot{x}_0 + y_0\omega_0}{x_0\omega_0 + \dot{y}_0} \tag{20}$$

$$\varphi_{02} = -\tan^{-1}\frac{\dot{x}_0 + y_0\omega_0}{x_0\omega_0 - \dot{y}_0} \tag{21}$$

To identify the type of extremum, it is required to calculate the second partial derivative of equation (17) with respect to each initial angular position, see equations (22) and (23). If the second partial derivative is greater than zero when inserting the value of the starting angular positions given by equations (20) and (21), the extremum is a minimum. If the second partial derivative is smaller than zero, the extremum is a maximum. Note, the signs of equations (22) and (23) alternate in multiples of π. This means that when equation (18) is at a minimum, equation (19) is at a maximum and vice versa. Therefore, to assure that both rotors start with (optimal) initial angular positions corresponding to maximum damping performance (minimum work done by the control force), π needs to be added to

equation (20) or (21) depending on the sign of equations (22) and (23). Hence, the optimal initial angular positions $\varphi_{01,o}$ and $\varphi_{02,o}$ are given by equations (24) and (25).

$$\frac{\partial^2 \Delta E}{\partial {\varphi_{01}}^2} = \frac{1}{2} m_c r \omega_0 \pi (\dot{x}_0 \sin\varphi_{01} - x_0 \omega_0 \cos\varphi_{01} - \dot{y}_0 \cos\varphi_{01} - y_0 \omega_0 \sin\varphi_{01}) \tag{22}$$

$$\frac{\partial^2 \Delta E}{\partial {\varphi_{02}}^2} = \frac{1}{2} m_c r \omega_0 \pi (-\dot{x}_0 \sin\varphi_{02} + x_0 \omega_0 \cos\varphi_{02} - \dot{y}_0 \cos\varphi_{02} - y_0 \omega_0 \sin\varphi_{02}) \tag{23}$$

$$\varphi_{01,o} = \begin{cases} \varphi_{01} & \text{for} \quad \dfrac{\partial^2 \Delta E}{\partial {\varphi_{01}}^2} > 0 \\ \varphi_{01} + \pi & \text{for} \quad \dfrac{\partial^2 \Delta E}{\partial {\varphi_{01}}^2} < 0 \end{cases} \tag{24}$$

$$\varphi_{02,o} = \begin{cases} \varphi_{02} & \text{for} \quad \dfrac{\partial^2 \Delta E}{\partial {\varphi_{02}}^2} > 0 \\ \varphi_{02} + \pi & \text{for} \quad \dfrac{\partial^2 \Delta E}{\partial {\varphi_{02}}^2} < 0 \end{cases} \tag{25}$$

3.2. Open-loop configuration

Applying the control forces from equations (7) and (8) to the free vibrations of the TDOF oscillator, the equations of motion (26) and (27) are formed, in which μ_c is the ratio of the control mass to total mass, see equation (28). The optimal initial angular positions $\varphi_{01,o}$ and $\varphi_{02,o}$ are utilized for the open-loop configuration of free vibrations of the TDOF oscillator. Solving these differential equations for the displacement responses of the TDOF oscillator yields equations (29) and (30) [7]. These equations characterize the trajectory of the TDOF while being damped by the control forces.

$$\ddot{x} + \omega_0^2 x = \frac{\mu_c}{2} r \omega_0^2 \left[\sin\left(\omega_0 t + \varphi_{02,o}\right) - \sin\left(\omega_0 t + \varphi_{01,o}\right)\right] \tag{26}$$

$$\ddot{y} + \omega_0^2 y = \frac{\mu_c}{2} r \omega_0^2 \left[\cos\left(\omega_0 t + \varphi_{02,o}\right) + \cos\left(\omega_0 t + \varphi_{01,o}\right)\right] \tag{27}$$

$$\mu_c = \frac{m_c}{m + m_c} \tag{28}$$

$$\begin{aligned} x(t) = {} & \frac{\dot{x}_0}{\omega_0} \sin(\omega_0 t) + x_0 \cos(\omega_0 t) + \frac{\mu_c r}{4} \{\sin(\omega_0 t)\left(\cos\varphi_{02,o} - \cos\varphi_{01,o}\right) + \cdots \\ & \omega_0 t\left[\cos\left(\omega_0 t + \varphi_{01,o}\right) - \cos\left(\omega_0 t + \varphi_{02,o}\right)\right]\} \end{aligned} \tag{29}$$

$$\begin{aligned} y(t) = {} & \frac{\dot{y}_0}{\omega_0} \sin(\omega_0 t) + y_0 \cos(\omega_0 t) + \frac{\mu_c r}{4} \{-\sin(\omega_0 t)\left(\sin\varphi_{02,o} + \sin\varphi_{01,o}\right) + \cdots \\ & \omega_0 t\left[\sin\left(\omega_0 t + \varphi_{02,o}\right) + \sin\left(\omega_0 t + \varphi_{01,o}\right)\right]\} \end{aligned} \tag{30}$$

Figure 3 shows a trajectory of the TDOF oscillator. The arrows depict the direction in which the TDOF oscillator is moving. The solid line shows the TDOF oscillator being effectively damped (positive active damping) and the dashed line shows the TDOF oscillator being re-excited (negative active damping). Note all initial states are normalized with respect to the initial displacement x_0. The unitless ratio $\mu_c r {x_0}^{-1}$ determines the decay rate. The higher this ratio becomes the larger the control force is; thus, the damping effect is larger.

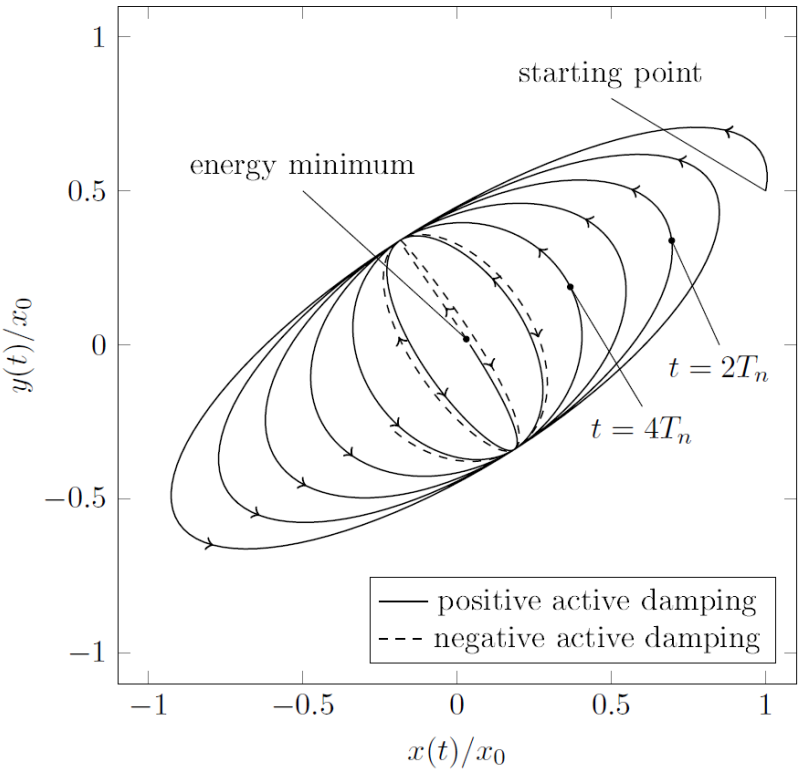

Figure 3: Open-loop trajectory of the TDOF oscillator with $\mu_c r {x_0}^{-1} = .06$, $y_0 = 0.5x_0$, $\dot{y}_0 = 0.5x_0\omega_0$ and $\dot{x}_0 = 0.1x_0\omega_0$

3.3. Target angular rotor positions

In subsection 3.2, the optimal initial angular positions, $\varphi_{01,o}$ and $\varphi_{02,o}$, were derived. These angular positions ensure that maximum damping performance for the free vibrations of the TDOF oscillator is achieved. This approach is adequate for the open-loop control of free vibrations. However, when additional factors such as external loadings, friction, or system imprecisions are considered, this open-loop control could lead to large inaccuracies [8]. A closed-loop configuration is, in such cases, more reliable and can be designed by continuously calculating optimal angular positions based on the states of the TDOF oscillator. This is done using the same method used for the calculation of the optimal initial angular rotor positions; however, now the initial states $(x_0, \dot{x}_0, y_0, \dot{y}_0)$ are replaced with the continuous states $(x(t), \dot{x}(t), y(t), \dot{y}(t))$, see equations (31)-(34). The continuously calculated optimal angular positions, $\varphi_{T1,o}(t)$ and $\varphi_{T2,o}(t)$, will henceforth be referred to as target angular positions. The damping direction defined by equation (9) is now, due to the time dependent target angular positions, able to change with respect to time and given by equation (35). As the damping direction is now time-dependent, the direction of the control force is required to change. This is done by allowing for small variations in the angular velocities.

$$\varphi_{T1}(t) = \tan^{-1}\frac{-\dot{x}(t) + y(t)\omega_0}{x(t)\omega_0 + \dot{y}(t)} \tag{31}$$

$$\varphi_{T2}(t) = -\tan^{-1}\frac{\dot{x}(t) + y(t)\omega_0}{x(t)\omega_0 - \dot{x}(t)} \tag{32}$$

$$\varphi_{T1,o}(t) = \begin{cases} \varphi_{T1}(t) & \text{for } \dfrac{\partial^2 \Delta E}{\partial \varphi_{T1}(t)^2} > 0 \\ \varphi_{T1}(t) + \pi & \text{for } \dfrac{\partial^2 \Delta E}{\partial \varphi_{T1}(t)^2} < 0 \end{cases} \tag{33}$$

$$\varphi_{T2,o}(t) = \begin{cases} \varphi_{T2}(t) & \text{for } \dfrac{\partial^2 \Delta E}{\partial \varphi_{T2}(t)^2} > 0 \\ \varphi_{T2}(t) + \pi & \text{for } \dfrac{\partial^2 \Delta E}{\partial \varphi_{T2}(t)^2} < 0 \end{cases} \tag{34}$$

$$\varphi_D(t) = \frac{\varphi_{T1,o}(t) - \varphi_{T2,o}(t)}{2} \tag{35}$$

3.4. Closed-loop control algorithm

The closed-loop configuration used for the tracking of the target angular positions is shown in figure 4. The TDOF oscillator provides the continuous states $x(t), \dot{x}(t), y(t), \dot{y}(t)$ which are then used to compute the target angular positions according to equations (33) and (34). The angular position error is then calculated by comparing the target angular positions $\varphi_{T1,o}(t)$ and $\varphi_{T2,o}(t)$ with the actual angular positions $\varphi_1(t)$ and $\varphi_2(t)$, see equation (36). The angular position errors $e_1(t)$ and $e_2(t)$ are then restricted to values between $-\pi$ and π to form the control errors $e_{c1}(t)$ and $e_{c2}(t)$. This ensures that the rotors are driven to the closest target angular position [4] [5]. The control error is then minimized using a combined closed-loop configuration for the angular position and an open-loop configuration for the angular velocity, see equation (37). The open-loop angular velocity configuration

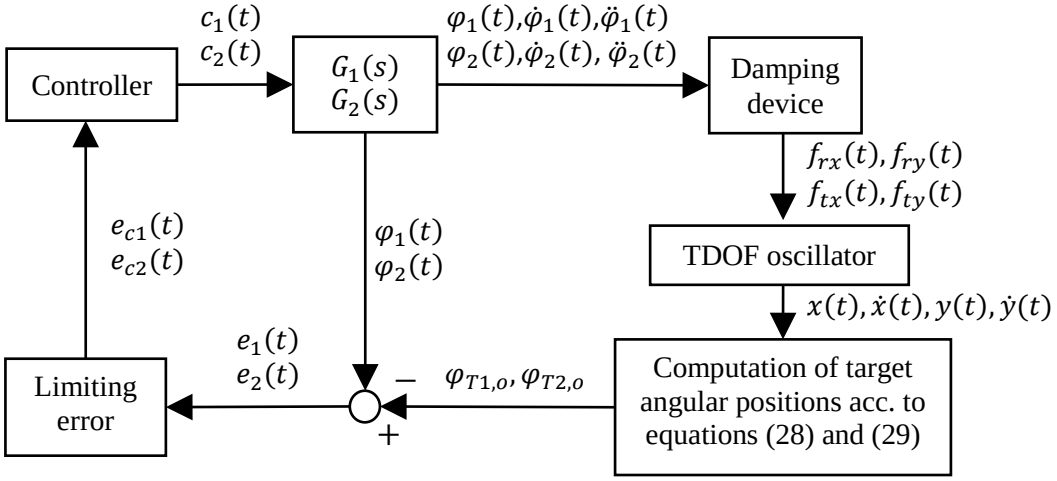

Figure 4: Closed-loop control algorithm.

is used to keep the angular velocity constant and equal to ω_0. This is realised by K_c and enables the proportional gain K_p to be smaller and simultaneously allows for adequately small control errors [8]. Therefore, the control efforts are given by equation (37). The proportional gain is tuned by hand and constant. Strictly proper transfer functions $G_1(s)$ and $G_2(s)$ with the form shown in equation (38) are used to simulate the dynamics of each rotor. The input of the transfer functions is the control effort and the output is the angular velocity of the corresponding rotor. Note a and b are constant values. Integrating and deriving the angular velocities with respect to time gives the angular positions and the

angular accelerations. By doing this, all states required to calculate the radial and tangential forces are available for the simulation, see figure 4.

$$e_1(t) = \varphi_{T1,o}(t) - \varphi_1(t) \qquad e_2(t) = \varphi_{T2,o}(t) - \varphi_2(t) \tag{36}$$

$$c_1(t) = e_{c1}(t)K_p + K_c \qquad c_2(t) = e_{c2}(t)K_p + K_c \tag{37}$$

$$G(s) = \frac{a}{s+b} \tag{38}$$

3.5. Numerical closed-loop simulations

The initial conditions from the open-loop configuration were also used for the numerical simulations performed with the closed-loop configuration. The additional variables for the controller and transfer function were set to: $a = b = 30$, $K_c = \omega_0 = 2\pi$ and $K_p = 5$. In figure 5, the responses of the TDOF oscillator together with the control errors and angular velocities of the rotors are shown for a length of $10T_n$.

Figure 5 shows that the vibrations in both x and y directions are effectively damped. Therefore, the total vibration amplitude $A(t)$ of the TDOF oscillator, given by equation (39), is reduced. At the beginning of the simulation, the control errors $e_{c1}(t)$ and $e_{c2}(t)$ rise slightly. This is due to the rotors having an initial angular velocity of zero. Once the rotors acquire the preferred angular velocity of ω_0, the control errors become small.

The control errors are small and the rotors have a mostly constant angular velocity equal to ω_0 until $t \approx 4T_n$. By this time, the vibrations in x direction have been damped to approximately half their original amplitude, whereas, in the same duration, the vibrations in y direction were only damped approximately 20%. This is due to the larger initial amplitude of the vibrations in x direction. At $t \approx 4T_n$, the vibrations in x and y direction have been damped to almost the same vibration amplitude and both degrees of freedom have a phase offset of 0.5π. Therefore, the trajectory of the TDOF oscillator is approximately circular, see the first subfigure of figure 5. To continue damping the vibrations, rotor 1 is required to accelerate strongly and hold a higher angular velocity while rotor 2 only varies its angular velocity slightly. The acceleration of the rotors produces additional tangential forces normal to the radial forces (control force). From $A(t)$, it can be seen that the vibrations are no longer smoothly damped. The tangential forces, mainly induced by rotor 1, slightly excite and then damp the vibrations leading to the stronger inconsistencies in $A(t)$.

The vibrations are damped until $t \approx 7T_n$, at which time the total vibration amplitude $A(t)$ starts to oscillate around 10% of the initial total vibration amplitude A_0. Starting at this point in time, rotor 2 no longer has an approximately constant angular velocity, but starts to accelerate strongly and acquires an angular velocity similar to rotor 1 by $t \approx 8.5T_n$.

$$A(t) = \left[x(t)^2 + \left(\frac{\dot{x}(t)}{\omega_0}\right)^2 + y(t)^2 + \left(\frac{\dot{y}(t)}{\omega_0}\right)^2\right]^{1/2} \tag{39}$$

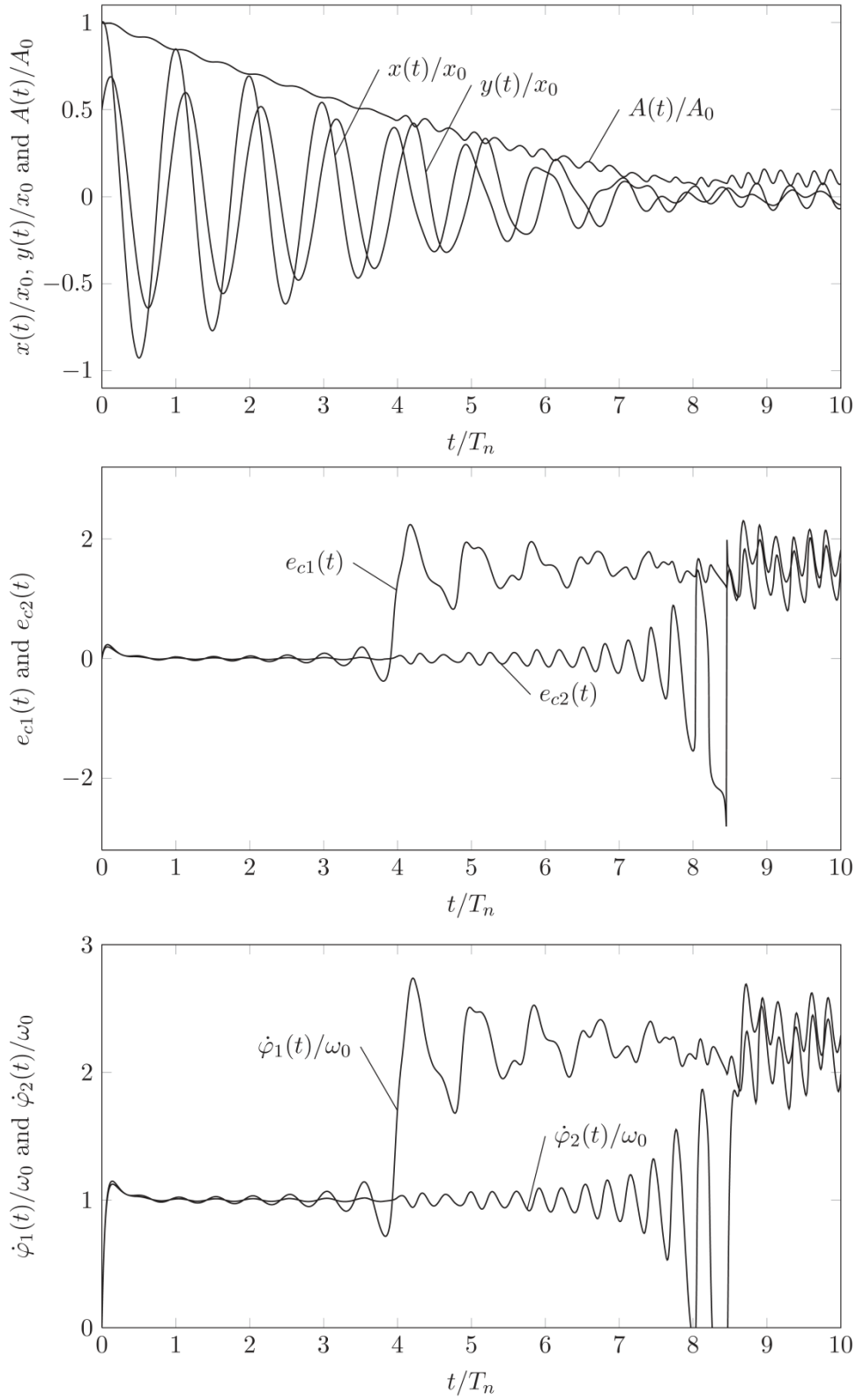

Figure 5: Closed-loop simulations with $\mu_c r {x_0}^{-1} = .06$, $y_0 = 0.5x_0$, $\dot{y}_0 = 0.5x_0\omega_0$ and $\dot{x}_0 = 0.1x_0\omega_0$

4. **Discussion**

In reality electrical motors would be used to accelerate the rotors. These motors would require more energy the more the rotors are required to accelerate. Using the open-loop configuration, the vibrations of the TDOF oscillator are re-excited after being originally damped. This and the fact that small imprecisions or changes in the modelling would lead to large errors is the reason why a closed-loop configuration was developed. However, although the vibrations are not re-excited when using a closed-loop configuration, two additional issues arise. When the trajectory of the TDOF oscillator becomes circular, one rotor is required to accelerate extremely and take on a higher angular velocity, while the other rotor accelerates slightly. The extreme acceleration of one of the rotors indicates that large tangential forces are required. The second issue is when the total vibration amplitude, $A(t)$, becomes too small. The device can continue to damp the vibrations of the TDOF oscillator, even after reaching the circular state, but once the total vibration amplitude reaches a certain small amplitude both rotors are required to accelerate. The acceleration of the rotors and the resulting tangential forces are unwanted as additional external energy would be required making the use of the presented device less economical. Introducing vibration amplitude thresholds, at which the presented device is turned on or off, may be a possibility to avoid these issues. This and other strategies on how to cope with these issues are subject of future work.

5. **Conclusions**

An active mass damper implementing the centrifugal forces produced by the rotation of two auxiliary masses for the vibration control of an oscillator with two translational degrees of freedom (TDOF) is presented. In a preferred mode of operation, both auxiliary masses rotate with the same nearly constant angular velocity in opposite directions producing a control force. By slightly varying the angular velocities, the direction of the control force can be changed. This allows for the vibration control in two TDOF.

A control algorithm was derived by minimizing the work done by the control force on the TDOF oscillator. This ensures that the control force is used to dissipate vibration energy and, thus damp the vibrations. For an open-loop configuration, an analytical solution was found. For a closed-loop configuration, it was shown that the control algorithm is effective; however, two issues arise. They are presented in the discussion and are subject of future work.

References

[1] Ekelund T 2000 Yaw control for reduction of structural dynamic loads in wind turbines *J. Wind Engineering and Industrial Aerodynamics* **85** 241-262

[2] Ming-Yi L, Wei-Ling C, Chia-Ren C and Shih-Sheng L 2002 Analytical and experimental research on wind-induced vibration in high-rise buildings with runed liequid column dampers *wind and structures* **6** 71-90

[3] Scheller J 2012 *Power-Efficient Active Structural Vibration Control by Twin Rotor Dampers* PhD thesis Hamburg University of Technology

[4] Bäumer R, Starossek U and Scheller J 2014, *Continuous State Feedback Control for Twin Rotor Damper* 9th Int. Conf. on Structual Dynamics June 30th-July 2nd Porta, Portugal

[5] Bäumer R and Starossek U. 2016 Active vibration control using centrifugal forces created by eccentrically rotating masses. ASME. *J. Vib. Acoust.*: doi:10.1115/1.4033358

[6] Clough R W and Penzien J 1993 *Dynamics of Structures* (New york: McGraw-Hill) 2nd edition

[7] Bronshtein I N and Semendyayev K A 1985 *Handbook of Mathematics* ed Grosche G and Ziegler V (Leipzig: Verlag Harri Deutsch, Thun and Frankfurt/Main)

[8] Franklin F F, Powell J D and Emami-Naeini A 2002 *Feedback Control of Dynamic Systems* (Upper Saddle River, NJ: Prentice Hall) 4th edition